Secure Systems Design and Technology Development. Veliko Tarnovo, Bulgaria
Proceedings of the International Scientific Conference, 2026. Volume II, 391-395

Scratch-Test Response of Color Laser-Marked AISI 304 Stainless Steel for a 7 × 7 Laser-Parameter Matrix

Imants Adijāns
Engineering Centre
Rezekne Academy of Riga Technical University
Rezekne, Latvia
Imants.Adijans@rtu.lv

***Abstract*—Durable color laser markings on stainless steel are attractive for traceability, product authentication, and identification of industrial components exposed to mechanical contact. In this work, the scratch-test response of nanosecond fiber-laser-marked AISI 304 stainless steel was evaluated for a 7 × 7 processing matrix. The laser-marking parameters were: average power P = 3–15 W and hatch spacing Δx = 40–100 µm, while the scanning speed, pulse repetition rate, pulse duration, and scanning strategy were kept constant at 100 mm/s, 500 kHz, 8 ns, and two passes (0°/90°), respectively. Scratch testing was performed with a CSEM REVETEST system using a Rockwell-type diamond indenter (tip radius 200 µm, cone angle 120°) under a progressive load from 0 to 30 N, with scratching oriented transverse to the raster direction. For all 49 conditions, the coefficient of friction μ and tangential force F_t were compared at a normal load F_n = 20 N and were benchmarked against the untreated surface.**

The untreated reference exhibited μ = 0.259 and F_t = 5.20 N. The most severe friction response was observed at P = 3 W and Δx = 40 µm, where μ increased to 0.406 (+56.7%). The lowest friction values were obtained at P = 3 W, Δx = 70 µm (μ = 0.225) and at P = 15 W, Δx = 100 µm (μ = 0.225), corresponding to reductions of about 13.2% relative to the untreated condition. Small hatch spacings (40–60 µm) required higher laser power to reduce friction, whereas Δx = 70 µm provided a comparatively stable low-friction window across the full power range. The results show that tribological response can be tuned by balancing interline overlap, local remelting, and the fraction of untreated surface retained between laser tracks.

Keywords*—*AISI 304 stainless steel, color laser marking, scratch test, tribology.

I. INTRODUCTION

Laser color marking of stainless steel offers a contactless and digitally controlled route for creating durable identification marks, serial data, and visually distinctive security features on metallic components. The technological interest in this process is driven not only by the possibility of obtaining stable oxide-based colors, but also by the need to preserve functional surface performance under service loading [1–6], [14], [15].

For AISI 304 stainless steel, previous studies have shown that the final appearance and morphology of a laser-marked surface depend strongly on thermal input, line overlap, and the balance between oxidation, local melting, and resolidification [1–6], [8], [10–13]. These parameters affect the continuity of the modified layer, the extent of remelting between adjacent tracks, the presence of untreated surface islands, and the resulting topography [10]–[13]. In applications where the marking is exposed to contact, sliding, or cleaning, such structural differences are expected to influence the tribological response of the surface. Recent studies have also addressed repeatability, optical-property variation, and the mechanical, chemical, and environmental stability of laser markings [13]–[15]. The broader laser-processing literature also shows that systematic multi-parameter optimization is essential for balancing thermal input and final surface quality, even when the substrate and wavelength differ from the present case [9-11], [13], [15], [16].

Scratch testing is a practical comparative method for assessing frictional response and surface failure development under progressive loading. At the same time, its interpretation must remain cautious, because the scratch response is affected by multiple material and test variables and is usually considered semi-quantitative rather than an absolute measure of adhesion or wear resistance [7]. For laser-marked stainless steel, this makes the scratch test especially useful for ranking process conditions within a fixed experimental framework.

The present work focuses on the scratch-test behaviour of a 7 × 7 matrix of double-pass nanosecond fiber-laser

Online ISSN 3044-7771
https://doi.org/10.68302/std2026.vol2.125

markings on AISI 304 stainless steel. The matrix varies two principal marking parameters—average laser power P and hatch spacing Δx—while keeping the remaining conditions constant. The objective is to determine how these parameters influence the coefficient of friction μ and the tangential force F_t at a normal load of 20 N, and to identify the most favourable process windows among the tested conditions.

II. Materials and Methods

A. *Material, sample preparation, and laser marking matrix*

All specimens were prepared from AISI 304 stainless steel with BA (bright annealed) surface finish. For the scratch-test study, a laser-marked plate with dimensions 150 × 150 × 1 mm was used. The surface was divided into 49 square fields arranged as a 7 × 7 matrix. Each field corresponded to one unique combination of laser power P and hatch spacing Δx. Before laser processing, the specimens were cleaned with isopropyl alcohol and dried under ambient laboratory conditions.

Laser marking was carried out using a ROFIN-SINAR PowerLine F20 Varia pulsed fiber-laser system (nominal wavelength approximately 1064 nm) equipped with a galvanometric scanning head and an F-theta lens. The effective focal length was 160 mm, the working distance was 184 mm, and the nominal focused spot diameter on the workpiece was approximately 40 µm. Marking was performed in focus.

The experimental matrix used constant marking conditions of scanning speed v = 100 mm/s, pulse repetition rate f = 500 kHz, pulse duration τ = 8 ns, and two scan repetitions executed at 0° and 90°. The variable factors were average laser power P = 3, 5, 7, 9, 11, 13, and 15 W and hatch spacing Δx = 40, 50, 60, 70, 80, 90, and 100 µm. For discussion purposes, the nominal power density was estimated from

$$q_s = \frac{4P}{\pi d^2} \quad (1)$$

which gives a range from 2.39×10^9 to 1.19×10^{10} W/m² for d = 40 µm.

TABLE I Experimental conditions and laser processing parameter matrix for colour marking of AISI 304 stainless steel prior to scratch testing

Item	Value	Comment
Material	AISI 304 stainless steel, BA finish	Untreated surface used as reference state
Marked plate	150 × 150 × 1 mm	49 square fields arranged as a 7 × 7 matrix
Laser system	ROFIN-SINAR PowerLine F20 Varia	Nanosecond pulsed fiber laser, ~1064 nm
Optics	F-theta lens, F = 160 mm	Working distance 184 mm; focused spot diameter $d \approx 40$ µm
Constant marking parameters	v = 100 mm/s; f = 500 kHz; τ = 8 ns	Two passes at 0° and 90°
Variable parameters	P = 3–15 W; Δx = 40–100 µm	Seven power levels × seven hatch spacings
Scratch tester	CSEM REVETEST	Rockwell-type diamond indenter
Indenter geometry	Tip radius 200 µm; cone angle 120°	Progressive load from 0 to 30 N
Scratch orientation	Transverse to raster direction	To reduce artefacts from inter-raster gaps
Quantitative comparison	μ and F_t extracted at F_n = 20 N	Untreated reference: μ = 0.259; F_t = 5.20 N

B. *Scratch-test methodology and data reduction*

Tribological measurements were performed with a CSEM REVETEST scratch-testing system. The indenter load increased progressively along the scratch path, while the normal load F_n, tangential force F_t, and filtered coefficient of friction

$$\mu = \frac{F_t}{F_n} \quad (2)$$

were continuously recorded. Scratching was performed transverse to the laser-raster orientation in order to minimise the influence of the indenter entering the interline spaces between adjacent laser tracks.

Optical images of the scratched regions were acquired using a digital reflected-light microscope at 400× magnification and were subsequently processed using Helicon Focus 7 to generate focus-stacked images with improved depth of field. In the present manuscript, however, the quantitative discussion is deliberately restricted to the measured μ and F_t values at F_n = 20 N, because this quantity is available consistently for the full 7 × 7 parameter matrix.

The untreated condition yielded μ = 0.259 and F_t = 5.20 N at F_n = 20 N. For each laser-marked field, the corresponding values at the same normal load were extracted from the uploaded measurement workbook. Since the current dataset contains one measurement per field and no replicate series, the analysis presented below is descriptive and comparative rather than statistical.

III. Results and Discussion

A. *Friction map for the 7 × 7 parameter matrix*

Figure 1 summarises the coefficient of friction measured at F_n = 20 N for all 49 laser-marked conditions. The strongest adverse response occurs at the smallest hatch spacing and the lowest laser power: P = 3 W and Δx = 40 µm produce μ = 0.406, which is 56.7% above the untreated reference. At the same hatch spacing, increasing the power to 15 W reduces μ to 0.250, showing that at dense raster spacing the tribological response is highly sensitive to the thermal input.

The most favourable values within the studied matrix are concentrated in two regions. The first is centred around Δx = 70 µm, where low-to-intermediate powers already yield μ in the interval 0.225–0.245. The second occurs at the largest hatch spacings (90–100 µm) combined with the highest powers (13–15 W), where μ drops to 0.225–0.240. These observations indicate that low friction is obtained either by a balanced intermediate spacing or by sufficiently high power at large spacings to enlarge the modified zone and reduce the heterogeneity between neighbouring tracks.

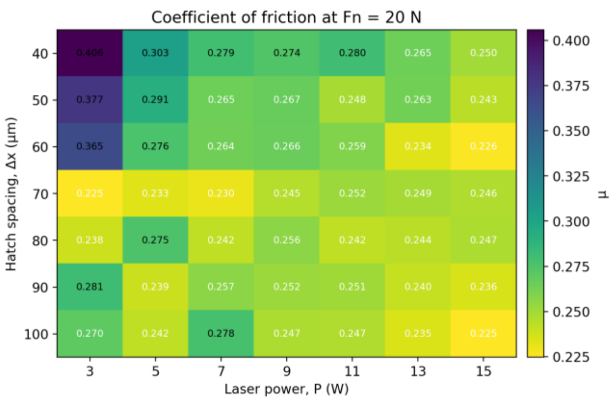

Fig. 1. Heatmap of the coefficient of friction μ at a normal load F_n = 20 N for the full 7 × 7 laser-parameter matrix.

B. *Effect of laser power at fixed hatch spacing*

The power-dependent trends are shown in Figure 2. For the small hatch-spacing group (Δx = 40–60 µm), increasing laser power causes a strong decrease in friction. At Δx = 40 µm, μ falls from 0.406 at 3 W to 0.250 at 15 W. At Δx = 50 µm and 60 µm, the same trend is preserved, with the friction minimum shifting toward the higher-power range. This behaviour is consistent with the transition from alternating laser-processed and unprocessed stripes toward a more continuous laser-affected surface as the thermal interaction zone becomes wider.

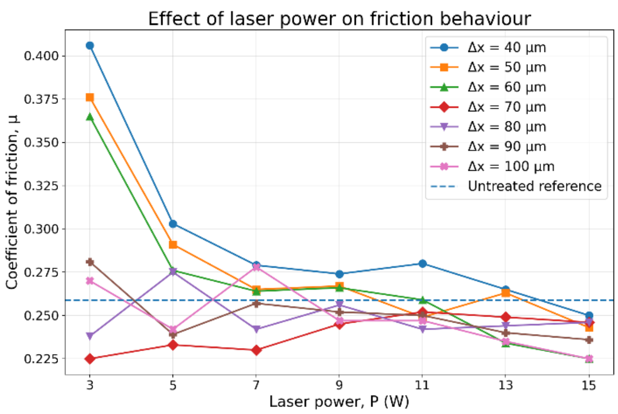

Fig. 2. Dependence of the coefficient of friction μ on laser power P for all investigated hatch spacings. The dashed line denotes the untreated reference.

The behaviour at Δx = 70 µm is different. Here the coefficient of friction is already low at 3 W (μ = 0.225) and remains within a narrow interval up to 15 W (μ = 0.246). This makes Δx = 70 µm the most robust hatch spacing in the present dataset, because it delivers comparatively low friction without the need for very high power.

At larger hatch spacings (Δx = 80–100 µm), the friction level is less monotonic with power. Low power leaves relatively large untreated regions between adjacent tracks and therefore tends to produce μ values close to, or slightly above, the reference. Increasing power enlarges the modified zone and reduces the response again, particularly for Δx = 90–100 µm and $P \geq 13$ W.

C. *Effect of hatch spacing at representative power levels*

Figure 3 shows the influence of hatch spacing at three representative powers. At P = 3 W, the response is strongly non-monotonic: μ is very high at Δx = 40–60 µm, reaches its minimum at Δx = 70 µm, and then rises again toward the reference level at Δx = 90–100 µm. This suggests that very low power is insufficient to homogenise the surface at small raster spacing, whereas excessively large spacing leaves too much untreated material between adjacent tracks.

At P = 9 W, the curve becomes flatter and most values lie close to the untreated condition, with a slight minimum near Δx = 70–100 µm. At P = 15 W, the hatch-spacing effect becomes more favourable at large Δx, and the lowest value is obtained at Δx = 100 µm. Higher power promotes wider tracks, stronger local remelting, and partial overlap, while larger hatch spacing preserves untreated islands. The best-performing conditions appear to balance these two tendencies rather than maximising either one separately.

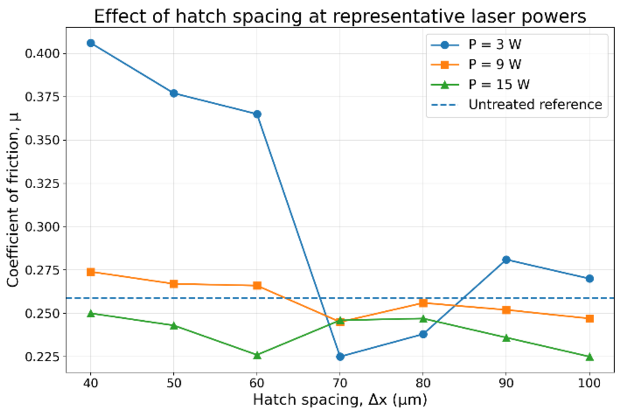

Fig. 3. Dependence of the coefficient of friction μ on hatch spacing Δx at representative power levels of 3, 9, and 15 W. The dashed line denotes the untreated reference.

D. Ranking of the most favourable and least favourable conditions

Table II ranks the lowest-friction conditions in the tested matrix and contrasts them with the untreated reference and the least favourable condition. Because the comparison was performed at a fixed normal load, the trend of the tangential force F_t mirrors the trend of μ, although F_t values are reported explicitly for completeness.

TABLE II REFERENCE CONDITION, MOST FAVOURABLE CONDITIONS, AND THE LEAST FAVOURABLE CONDITION AT $F_N = 20$ N

Category	Δx (µm)	P (W)	μ	F_t (N)	$\Delta\mu$ vs ref (%)
Untreated reference	—	—	0.259	5.20	+0.0
Low-friction rank 1	70	3	0.225	4.56	-13.2
Low-friction rank 2	100	15	0.225	4.64	-13.2
Low-friction rank 3	60	15	0.226	4.60	-12.7
Low-friction rank 4	70	7	0.230	4.68	-11.2
Low-friction rank 5	70	5	0.233	4.80	-9.9
Least favourable	40	3	0.406	8.24	+56.7

E. Interpretation and limitations

The friction trends are interpreted in terms of the relative proportions of laser-modified and unmodified surface regions, the degree of interline overlap, and the presence of local remelting. At very small hatch spacings and low power, the surface remains strongly heterogeneous and friction increases markedly. At higher power, the modified zones broaden and the surface becomes more continuous, which lowers friction. At excessively large spacings and low power, the untreated fraction dominates and the response approaches that of the initial BA surface.

The present paper should, however, be read with an important limitation in mind. Although scratch testing can in principle be used to determine critical loads for crack initiation and failure, the current analysis is restricted to the quantitatively available outputs μ and F_t at $F_n = 20$ N. Therefore, the conclusions below identify favourable parameter windows within this specific comparative experiment rather than universal optimum conditions.

F. Representative surface morphologies and their relation to friction

Figure 4 presents representative optical images used to relate surface morphology to the scratch-test friction response of laser-marked AISI 304. The untreated BA surface (Fig. 4a) serves as the reference. In the least favourable case, $P = 3$ W and $\Delta x = 40$ µm (Fig. 4b), the surface is strongly heterogeneous, with a pronounced contrast between laser-affected and less affected regions. This condition also produced the highest coefficient of friction in the tested matrix, indicating that an irregular and discontinuous surface morphology promotes unstable contact during scratching.

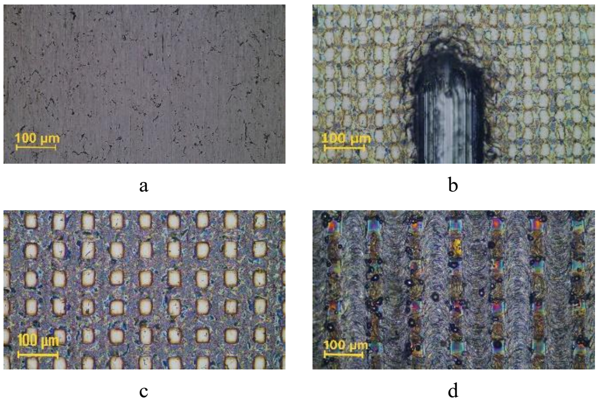

Fig. 4. Representative surface morphologies and their relation to scratch-test friction response: (a) untreated AISI 304 BA surface; (b) heterogeneous morphology and representative scratch track for $P = 3$ W and $\Delta x = 40$ µm; (c) representative morphology for $P = 5$ W and $\Delta x = 70$ µm; (d) representative morphology for $P = 15$ W and $\Delta x = 100$ µm.

In contrast, the surfaces obtained at $P = 5$ W and $\Delta x = 70$ µm (Fig. 4c) and at $P = 15$ W and $\Delta x = 100$ µm (Fig. 4d) show a more balanced and continuous morphology. The former is representative of the favourable parameter window around $\Delta x \approx 70$ µm, while the latter reflects stronger but more spatially uniform laser interaction at high power and large hatch spacing. The representative images support the conclusion that low power combined with small hatch spacing leads to increased heterogeneity and higher friction, whereas intermediate hatch spacing around 70 µm or large hatch spacing combined with high power provides a more favourable surface state for reduced friction.

IV. CONCLUSIONS

- A 7 × 7 scratch-test map was established for double-pass nanosecond fiber-laser markings on AISI 304 stainless steel by varying laser power $P = 3$–15 W and hatch spacing $\Delta x = 40$–100 µm under otherwise constant processing conditions.
- The untreated reference surface exhibited $\mu = 0.259$ and $F_t = 5.20$ N at $F_n = 20$ N. The highest-friction condition was $P = 3$ W and $\Delta x = 40$ µm ($\mu = 0.406$), whereas the lowest values were obtained at $P = 3$ W, $\Delta x = 70$ µm and $P = 15$ W, $\Delta x = 100$ µm ($\mu \approx 0.225$).
- For small hatch spacings (40–60 µm), increasing laser power substantially reduced friction, indicating that stronger thermal interaction and wider modified tracks mitigate the adverse effect of a highly heterogeneous surface. In contrast, $\Delta x = 70$ µm provided the most stable low-friction behaviour across the full power range.
- The most favourable process windows among the tested conditions were identified as: (i) intermediate

hatch spacing around Δx = 70 µm, especially at 3–7 W; and (ii) large hatch spacings of 90–100 µm combined with high power of 13–15 W. These regimes reduced both μ and F_t relative to the untreated reference.

- Because the dataset is descriptive, the reported trends should be treated as a practical ranking of the investigated conditions. Nevertheless, the results provide a clear basis for selecting laser-marking parameters when friction-sensitive and mechanically durable color markings are required on AISI 304 stainless steel.
- Future work should include replicate scratch tests, critical-load analysis from scratch-track damage, and correlation of friction with roughness, oxide-layer chemistry, and corrosion behaviour.

References

[1] Y. Lu, X. Shi, Z. Huang, T. Li, M. Zhang, J. Czajkowski, T. Fabritius, M. Huttula, and W. Cao, "Nanosecond laser coloration on stainless steel surface," *Sci. Rep.*, vol. 7, Art. no. 7092, 2017, doi: https://doi.org/10.1038/s41598-017-07373-8.

[2] R. Linggamm, M. M. Quazi, M. N. Bashir, M. H. Aiman, A. Qaban, F. Dave, and M. M. Ali, "A review on the formation of colors on SS304 stainless steel induced by laser color marking technique," *J. Adv. Technol. Eng. Res.*, vol. 7, no. 2, pp. 1-26, 2021, doi: https://doi.org/10.20474/jater-7.2.1.

[3] P. Tsvyatkov, E. Yankov, L. Lazov, E. Teirumnieks, and E. Teirumnieka, "Color marking of stainless steel and titanium with the laser oxidation method," *Environ. Technol. Resour., Proc. Int. Sci. Pract. Conf.*, vol. 3, pp. 363-369, 2024, doi: https://doi.org/10.17770/etr2023vol3.7318.

[4] L. Lazov, N. Angelov, E. Yankov, T. Karadzhov, D. Pulov, and D. Dichev, "Influence of laser processing parameters on surface roughness and color formation in the marked zone," *Materials*, vol. 18, no. 21, Art. no. 5037, 2025, doi: https://doi.org/10.3390/ma18215037.

[5] A. Schkutow and T. Frick, "Laser color marking of stainless steel - Investigation of the fluence-dependent and thermal mechanisms in generating laser induced surface modifications," *Procedia CIRP*, vol. 124, pp. 661-664, 2024, doi: https://doi.org/10.1016/j.procir.2024.08.196.

[6] X. Wang, Z. Xue, X. Qin, K. Song, D. Liu, and X. Wan, "Enhancement of laser-induced surface coloring through laser double-scan method," *Opt. Laser Technol.*, vol. 175, Art. no. 110738, 2024, doi: https://doi.org/10.1016/j.optlastec.2024.110738.

[7] S. J. Bull and E. G. Berasetegui, "An overview of the potential of quantitative coating adhesion measurement by scratch testing," *Tribol. Int.*, vol. 39, no. 2, pp. 99-114, 2006, doi: https://doi.org/10.1016/j.triboint.2005.04.013.

[8] M. Švantner, M. Kučera, E. Smazalová, Š. Houdková, and R. Čerstvý, "Thermal effects of laser marking on microstructure and corrosion properties of stainless steel," *Appl. Opt.*, vol. 55, no. 34, pp. D35-D45, 2016, doi: https://doi.org/10.1364/AO.55.000D35.

[9] I. Kubovský, Ľ. Krišťák, J. Suja, M. Gajtanska, R. Igaz, I. Ružiak, and R. Réh, "Optimization of parameters for the cutting of wood-based materials by a CO2 laser," *Appl. Sci.*, vol. 10, no. 22, Art. no. 8113, 2020, doi: https://doi.org/10.3390/app10228113.

[10] A. J. Antończak, D. Kocoń, M. Nowak, P. Kozioł, and K. M. Abramski, "Laser-induced colour marking—Sensitivity scaling for a stainless steel," *Applied Surface Science*, vol. 264, pp. 229–236, 2013, doi: https://doi.org/10.1016/j.apsusc.2012.09.178.

[11] V. Veiko *et al*., "Controlled oxide films formation by nanosecond laser pulses for color marking," *Optics Express*, vol. 22, no. 20, pp. 24342–24347, 2014, doi: https://doi.org/10.1364/OE.22.024342.

[12] E. H. Amara, F. Haïd, and A. Noukaz, "Experimental investigations on fiber laser color marking of steels," *Applied Surface Science*, vol. 351, pp. 1–12, 2015, doi: https://doi.org/10.1016/j.apsusc.2015.05.095.

[13] G. Odintsova *et al*., "Investigation of production related impact on the optical properties of color laser marking," *Journal of Materials Processing Technology*, vol. 274, art. 116263, 2019, doi: https://doi.org/10.1016/j.jmatprotec.2019.116263.

[14] D. Roozbahani, M. Alizadeh, H. Handroos, and A. Salminen, "Color Laser Marking: Repeatability, Stability and Resistance Against Mechanical, Chemical and Environmental Effects," *IEEE Access*, vol. 8, pp. 214196–214208, 2020, doi: https://doi.org/10.1109/ACCESS.2020.3040744.

[15] Y. Geng, J. Li, and C. Lu, "Experimental and numerical investigations on color stability of laser color marking," *Optics and Lasers in Engineering*, vol. 159, art. 107225, 2022, doi: https://doi.org/10.1016/j.optlaseng.2022.107225.

[16] S. Butkus *et al*., "High-Contrast Marking of Stainless-Steel Using Bursts of Femtosecond Laser Pulses," *Micromachines*, vol. 14, no. 1, art. 194, 2023, doi: https://doi.org/10.3390/mi14010194.